Luttinger-Kohn Hamiltonian and coherent excitation of the valence-band holes

A. Dargys*
Semiconductor Physics Institute, A. Goštauto 11, 2600 Vilnius, Lithuania
(Received 26 June 2002; published 29 October 2002)

Control of intervalence band transitions by femtosecond infrared pulses is studied as an initial value problem using the Luttinger-Kohn Hamiltonian and genetic algorithm. It is shown that initial phase relations between degenerate valence-band wave functions are important if excitation of the valence band by optimized pulses is fast enough. If the excitation is switched on and off slowly, the influence of phase relations on the intervalence band transition probabilities is negligible. Physical interpretation of the initial phase relations is presented. It is shown that phase differences between degenerate heavy-mass, light-mass, and spin-orbit split-off band wave functions of the Luttinger-Kohn Hamiltonian are connected with finite magnitude of hole spin projections. This property may find an application in the ultrafast spintronics.

DOI: 10.1103/PhysRevB.66.165216 PACS number(s): 78.47.+p, 42.65.Sf, 42.65.Pc

I. INTRODUCTION

Luttinger-Kohn (LK) Hamiltonian[1,2] is frequently used to describe hole properties at top of the valence band of most technologically important semiconductors, including elementary semiconductors, III-V compounds, and their alloys. Its popularity is connected with a small number of empirical parameters needed to represent complex valence-band structure in normal and strained semiconductors,[2,3] energy spectra of shallow acceptors and excitons,[4–7] and quantum properties of nanostructures.[8–12] The LK Hamiltonian is also frequently used in the analysis of hole intervalence transition properties, optical selection rules, absorption anisotropy, etc. in infrared (IR) radiation fields.[13–18] In this paper we shall be interested in the excitation of valence-band holes by high-intensity femtosecond IR laser fields.

In general, two modes of behavior of the valence-band holes under intense laser field irradiation are to be distinguished. When laser pulse is long, dissipation dominates in hole intervalence transition dynamics and, as a result, spectral hole is burnt out in hole distribution function at resonance energy. In essence, the effect is related with a disbalance between in and out hole scattering rates brought about by high intensity laser radiation. The properties of the spectral hole in *p*-type semiconductors were analyzed by Boltzmann equation,[19,20] density matrix equation,[21] or by simulating hole dynamics with Monte Carlo method.[22] In an opposite case, when laser pulse is shorter than average hole collision time with lattice phonons or imperfections, valence band mixing by strong electric field of IR radiation predominates. Earlier it was shown that such mixing induces intervalence Rabi oscillations[23] and may contribute to additional intervalence-band-tunneling noise in *p*-type semiconductors.[24]

From the perspective of semiconductor quantum device application, of all possible quantum coherence effects, an ultrafast control of population transfer between energy bands or impurity atomic levels is thought to be the most promising one. The possibility of ultrafast quantum control in quantum wells was shown by Krause *et al.*[25] Recently, it was shown that optical pulses of minimal energy exist, which can coherently transfer the carrier between energy bands in extremely short time limited by the Heisenberg time-energy uncertainty relation.[26] Characteristic population inversion patterns in the Brillouin zone are generated by such ultrashort pulses.[27,28] In papers[29,30] it was demonstrated that coherent all-optical injection of spin-polarized currents can be achieved if relative phases of the exciting lasers are controlled. In the present paper it will be shown that phase relations between degenerate valence-band wave functions can also play an important role in the coherent evolution of the hole state vector and in the final excitation probabilities. This fact may be important in the quantum control problems and in selecting an optimal excitation pulse.

This paper is organized as follows. In Sec. II basic equations are introduced. In Sec. III results of numerical experiments with optimized ultrashort pulses are presented. The results are limited only to optimal excitation of split-off band of *p*-GaAs in low doping limit. The discussion on macroscopic interpretation of the phase relations between degenerate or close to degenerate valence-band wave functions, when spin-orbit interaction is strong, is given in Sec. IV.

II. CALCULATIONAL METHODS

General form of the six-band LK Hamiltonian that consists of two terms,

$$\hat{H}_{LK}=\hat{H}_0+\hat{H}_1 \tag{1}$$

was used in the simulation, where $\hat{H}_0$ is the main term that represents doubly degenerate heavy-mass (h), light-mass (l), and split-off (s) bands. The second term $\hat{H}_1$ takes into account small splitting of doubly degenerate bands due to the absence of inversion symmetry in III-V compounds. The matrix $\hat{H}_0$ is made up of quadratic in wave vector $\mathbf{k}=(k_x,k_y,k_z)$ elements, where k_i's are referenced with respect to crystallographic axes. In the spinor basis $|J,m\rangle$, in the order $|\frac{3}{2},\frac{3}{2}\rangle,|\frac{3}{2},\frac{1}{2}\rangle,|\frac{3}{2},-\frac{1}{2}\rangle,|\frac{3}{2},-\frac{3}{2}\rangle,|\frac{1}{2},\frac{1}{2}\rangle,|\frac{1}{2},-\frac{1}{2}\rangle$, it is

$$\hat{H}_0=\begin{pmatrix} P+Q & L & M & 0 & \frac{i}{\sqrt{2}}L & -i\sqrt{2}M \\ L^\dagger & P-Q & 0 & M & -i\sqrt{2}Q & i\sqrt{\frac{3}{2}}L \\ M^\dagger & 0 & P-Q & -L & -i\sqrt{\frac{3}{2}}L^\dagger & -i\sqrt{2}Q \\ 0 & M^\dagger & -L^\dagger & P+Q & -i\sqrt{2}M^\dagger & -\frac{i}{\sqrt{2}}L^\dagger \\ -\frac{i}{\sqrt{2}}L^\dagger & i\sqrt{2}Q & i\sqrt{\frac{3}{2}}L & i\sqrt{2}M & P+\Delta & 0 \\ i\sqrt{2}M^\dagger & -i\sqrt{\frac{3}{2}}L^\dagger & i\sqrt{2}Q & \frac{i}{\sqrt{2}}L & 0 & P+\Delta \end{pmatrix}, \tag{2}$$

where $P=(\gamma_1/2)(k_x^2+k_y^2+k_z^2)\equiv(\gamma_1/2)k^2$, $Q=(\gamma_2/2)(k_x^2+k_y^2-2k_z^2)$, $L=-i\sqrt{3}\gamma_3 k_z(k_x-ik_y)$, $M=(\sqrt{3}/2)\gamma_2(k_x^2-k_y^2)-i\sqrt{3}\gamma_3 k_x k_y$, and $i=\sqrt{-1}$. Atomic units (a.u.) are used throughout. The Hamiltonian $\hat{H}_0$ is characterized by three empirical parameters γ_1, γ_2, and γ_3, and strength Δ of the spin-orbit splitting between Γ_8 and Γ_7 bands at point $\mathbf{k}=0$. The eigenvalues of Eq. (2) yield nonparabolic, nonspherical, and doubly degenerate heavy-mass, light-mass, and split-off band dispersion laws that describe dependence of the hole energy in a particular band as a function of the wave vector $\mathbf{k}$.

The correction term $\hat{H}_1$ is linear in k_i's. It lifts off the double degeneracy and in the above mentioned ordering of $|J,m\rangle$ basis has the following form:[31]

$$\hat{H}_1=\begin{pmatrix} 0 & -i\kappa & -\lambda & i\sqrt{3}\kappa^\dagger & \mu & -i\nu \\ i\kappa^\dagger & 0 & i\sqrt{3}\kappa & \lambda & 0 & \sqrt{3}\mu \\ -\lambda & -i\sqrt{3}\kappa^\dagger & 0 & -i\kappa & -\sqrt{3}\mu^\dagger & 0 \\ -i\sqrt{3}\kappa & \lambda & i\kappa^\dagger & 0 & i\nu & -\mu^\dagger \\ \mu^\dagger & 0 & -\sqrt{3}\mu & -i\nu & 0 & 0 \\ i\nu & \sqrt{3}\mu^\dagger & 0 & -\mu & 0 & 0 \end{pmatrix}. \tag{3}$$

In Eq. (3), $\kappa=(c/2)(k_x+ik_y)$, $\lambda=ck_z$, $\mu=(c'/2\sqrt{2})(k_x+ik_y)$, and $\nu=(c'/\sqrt{2})k_z$. The empirical coefficient c couples Γ_8 states, while coefficient c' couples Γ_7 states to Γ_8 states. The unitary transformation matrix that connects matrix (3) and the corresponding matrix in Ref. 31 is

$$\begin{pmatrix} i & 0 & 0 & 0 & 0 & 0 \\ 0 & 0 & 0 & -1 & 0 & 0 \\ 0 & -1 & 0 & 0 & 0 & 0 \\ 0 & 0 & -i & 0 & 0 & 0 \\ 0 & 0 & 0 & 0 & i & 0 \\ 0 & 0 & 0 & 0 & 0 & -1 \end{pmatrix}.$$

To find hole intervalence dynamics in an arbitrarily varying electromagnetic field the following Schrödinger equation for six-component state vector $|\psi\rangle$ was solved numerically:

$$i\frac{\partial|\psi\rangle}{\partial t}=\left(\hat{H}_0+\frac{\mathbf{F}(t)}{i}\frac{\partial}{\partial\mathbf{k}}\right)|\psi\rangle, \tag{4}$$

where $\mathbf{F}(t)$ is the time-dependent electric field of the electromagnetic radiation. The Schrödinger system can be reduced to full derivatives, if one notes that equation of motion for the hole wave vector

$$d\mathbf{k}/dt=\mathbf{F}(t) \tag{5}$$

at the same time is the characteristic equation of the system (4). Optimal, femtosecond duration pulses were obtained after incorporation of the system (4) into genetic algorithm (GA).[32,33]

With the optimal electric field $\mathbf{F}(t)$ known, in a real evolution where dissipation influences the coherence of intervalence transitions, the hole dynamics was simulated with the help of dynamical equation for 6×6 density matrix

$$i\frac{\partial\hat{\rho}}{\partial t}=[\hat{H}_{LK},\hat{\rho}]+i\hat{T}\mathcal{L}_{relax}\hat{T}^{-1}. \quad (6)$$

Here, $\mathcal{L}_{relax}$ is the relaxation operator in the energy representation and $\hat{T}$ is the unitary transformation operator that relates energy and spinor basis $|J,m\rangle$ representations. In Eq. (6) the electric field takes effect indirectly through equation of motion (5) for the hole wave vector. In the absence of dissipation, when $\mathcal{L}_{relax}$ is unimportant, the density matrix (6) and Eq. (5) yield the same results as the Schrödinger system (4). Nonetheless, from the computational point of view both systems are not equivalent. In the Schrödinger system the integration is over six coupled equations, while in the density-matrix system the integration is over 21 coupled complex elements of $\hat{\rho}(t)$. The remaining nondiagonal elements in $\hat{\rho}(t)$ can be found by complex conjugation, including the dissipative case.

The relaxation operator was represented as a sum of two terms[34]

$$\mathcal{L}_{relax}=-\{\hat{R},\hat{\sigma}\}+\hat{\sigma}_e, \quad (7)$$

where $\hat{\sigma}$ is the time-dependent density matrix in the energy representation and $\hat{\sigma}_e$ is the corresponding equilibrium matrix. $\hat{R}$ is the scattering operator. The curly brackets denote the anticommutator: $\{\hat{R},\hat{\sigma}\}=\hat{R}\hat{\sigma}+\hat{\sigma}\hat{R}$. The matrix $\hat{\sigma}$ is connected with the density matrix $\hat{\rho}$ in Eq. (6) by the same unitary transformation,

$$\hat{\sigma}(t)=\hat{T}^{-1}(t)\hat{\rho}(t)\hat{T}(t). \quad (8)$$

The time-dependent unitary matrix $\hat{T}(t)$ at the same time diagonalizes the LK Hamiltonian at all moments t,

$$\hat{H}_d=\hat{T}^{-1}\hat{H}_{LK}\hat{T}=\mathrm{diag}\{E_{s1},E_{s2},E_{l1},E_{l2},E_{h1},E_{h2}\}, \quad (9)$$

where the diagonal elements in the matrix (9) represent dispersion laws of the respective bands. The knowledge of $\hat{\rho}(t)$ and $\hat{T}(t)$ is sufficient to find the dynamics of the hole population in all six valence bands as well as time dependence of nondiagonal terms (coherences) of $\hat{\sigma}$ with the help of Eq. (8).

In the relaxation matrix (7), the band population relaxations and decoherences due to hole momentum scattering by acoustical, optical, and screened polar optical phonons, with intraband and interband hole transfer for all three bands, were taken into account. Screened ionized impurity scattering was also included, which may be important at low lattice temperatures. The final scattering angles were determined by Monte Carlo rejection method proposed in Ref. 35. By accepting only those final states that have the angular distribution that satisfies the warping and valence-band wave function overlap conditions, one can obtain the correct scattering rates in the matrix (7). The hole spin relaxation was included through elastic and nonelastic momentum scattering only. In general, the data on hole spin relaxation are scare, although, it is well established that, contrary to electron-spin relaxation, the hole spin relaxation is fast and lies in the picosecond time scale.[36,37] In the present calculations, it was assumed that only longitudinal relaxation of the hole spin due to hole momentum scattering is important, i.e., only diagonal elements were included in $\hat{R}$. The transverse spin relaxation was neglected. It was assumed that before application of the laser pulse the hole distribution was in a thermal equilibrium with semiconductor lattice. Since matrix $\hat{\sigma}$ is in energy representation, its diagonal elements give the probabilities to find the hole in the ith band. The Boltzmann distribution was used to calculate the initial occupation probability

$$p_i(\mathbf{k_0})\equiv(\hat{\sigma}_e)_{ii}=\frac{e^{-E_i(\mathbf{k_0})/kT}}{\sum_i e^{-E_i(\mathbf{k_0})/kT}} \quad (10)$$

of the ith band at initial wave vector $\mathbf{k_0}$. In Eq. (10), T is the lattice temperature and the sum runs over all bands: $i=s1,s2,l1,l2,h1,h2$.

The shape of the optimal electric field $\mathbf{F}(t)=[F_x(t),F_y(t),F_z(t)]$ that controls motion of the wave vector in Eq. (5) was approximated by rather general empirical formula

$$F_i(t)=F_{i1}\sin[\omega(t-t_d)+\alpha(t-t_d)^2+\varphi_i]\times\frac{\exp\left(-\sum_{n=2}^{4}a_n\tau^n\right)}{1+\mathrm{sgn}(t-t_d)a_1\tau^m}, \quad (11)$$

where $\tau=(t-t_d)/t_f$. Here, t_d is the delay time and t_f is the final simulation time. In the optimization, $t_d=t_f/2$ was used.

TABLE I. Parameters of lattice, valence band, and hole-phonon interaction in GaAs (Ref. 38).

Quantity	Unit	Value
Lattice constant, a	nm	0.565
Density, ρ	g/cm^3	5.316
Sound velocity, s	m/s	3860
Dielectric permittivity		
static, ε_0		12.8
high frequency, ε_∞		10.92
Optical phonon energy, $\hbar\omega_{op}$	eV	0.035
Valence band parameters		
γ_1		6.85
γ_2		2.1
γ_3		2.9
Spin-orbit splitting, Δ	eV	0.341
Split-off band mass, m_s		0.154
Acoustic deformation potential, E_1	eV	5.6
Optical deformation potential, DK	eV/m	1.26×10^{11}
Heavy-light band linear coupling, c	eV m	0.36×10^{-12}
Linear coupling to split-off band, c'	eV m	$c/2$
Inverse screening length, β	m^{-1}	10^8
Ionized impurity concentration, N_I	cm^{-3}	10^{15}

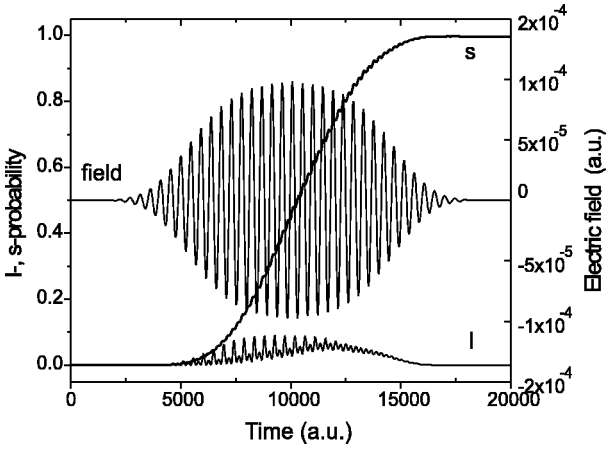

FIG. 1. Time dependence of π-type pulse generated by GA and hole excitation probability to split-off (s) and light-mass (l) band. $-k_{x0}=k_{y0}=k_{z0}=0.2$ nm^{-1}. $t_f=20\,000$ a.u.$=484$ fs. 1×10^{-4} a.u. field$=5.14\times10^5$ V/cm.

In formula (11), eight parameters—amplitude F_{i1}, angular frequency ω, chirping coefficient α, initial phase φ_i, and four parameters a_n that control the shape of an envelope function of the field—were varied simultaneously within some fixed ranges by the GA. The standard GA[32,33] was used to find an optimal set of the parameters. The optimality criterion (or fitness of the corresponding chromosome in the GA parlance) that determines pulse shape was evaluated with

$$\Phi_i=\max\left[p_i(t_f)-a\int_0^{t_f}|\mathbf{F}(t)|^2dt\right]. \tag{12}$$

The first term in Eq. (12) requires the probability to find the hole in the ith band, to be maximal at the final time of the simulation. The second term in Eq. (12) is the penalty function, which requires the energy of the pulse to be minimal. The coefficient a is the positive constant assumed beforehand. Thus, to maximize the fitness (12) the GA must find the best combination of eight parameters in the driving field (11). In this paper only optimal hole transitions to split-off band of GaAs, which satisfy criterion (12) will be presented. The material parameters of GaAs used in the simulation are given in Table I.

III. OPTIMIZED *H-S* TRANSITIONS

Figure 1 shows electric-field pulse shape generated by GA and Schrödinger system (4), and the resulting time-dependence of probabilities $p_s(t)$ and $p_l(t)$ to detect the hole in the split-off and light-mass bands at the moment t. The field $\mathbf{F}=(F_x,0,0)$ was linearly polarized and parallel to $\langle100\rangle$ crystallographic axes. At $t=0$ the hole was in the heavy-mass band and possessed initial wave vector $\mathbf{k_0}=0.2\times(-1,1,1)$ nm^{-1}. For this wave vector the Hamiltonian Eq. (2) yields the interband resonance energies $E_{lh}(\mathbf{k_0})=E_l(\mathbf{k_0})-E_h(\mathbf{k_0})=48.6$ meV and $E_{sh}(\mathbf{k_0})=E_s(\mathbf{k_0})-E_h(\mathbf{k_0})=371$ meV. The frequency ω selected by the GA in Eq. (11) is 0.013 62 a.u. This value corresponds to photon energy $\hbar\omega=370.6$ meV that is very close to resonance energy $E_{sh}(\mathbf{k_0})$.

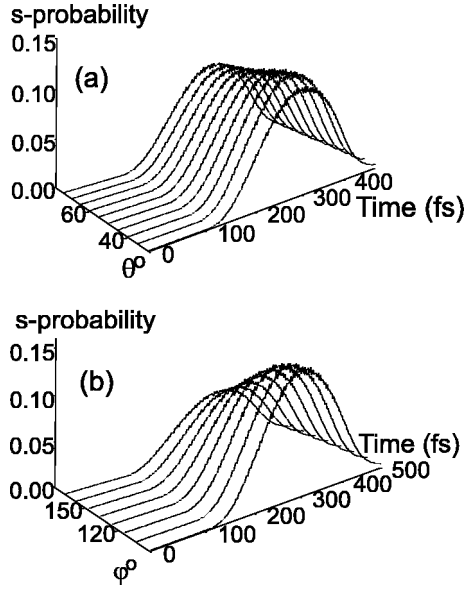

FIG. 2. Evolution of hole distribution at various initial (a) polar and (b) azimuthal angles of the wave vector $\mathbf{k_0}$ under same exciting field as in Fig. 1. $|\mathbf{k_0}|=0.347$ nm^{-1}. $T=300$ K.

Linear-$\mathbf{k}$ corrections were neglected in Fig. 1 and initial phase difference $\Delta\phi_{hh}$ between degenerate heavy-mass wave functions was assumed zero. The calculations then were repeated with $\Delta\phi_{hh}=\pi/2$ as well as with some intermediate $\Delta\phi_{hh}$ values. In all cases it was found that, independent of initial $\Delta\phi_{hh}$, the magnitude of the final transition probability $p_s(t_f)$ after integration of the Schrödinger system practically (up to three significant digits at final time $t_f=484$ fs) was the same. From this we conclude that the results of numerical simulation shown in Fig. 1 correspond to vertical interband transitions and are in accordance with the well-known adiabatic approximation theory, where phase relations are considered to have negligible influence on observables if perturbation is switched on and off slowly.[39] Since in the integration of the Schrödinger system no approximations were made, in Fig. 1 one can also see fast oscillations superimposed on the slowly varying transition probabilities. They are in phase with the harmonically varying field. Normally, the fast oscillations are absent if solutions are obtained by approximate methods, for example, within the rotating wave approximation. The calculations shown in Fig. 1 then were repeated with the density-matrix equation (6) using the same shape of the electric field as in Fig. 1 and with dissipation term switched off. Exactly the same time dependence of probabilities was observed in this case too, if the phase differences in nondiagonal matrix elements that relate heavy-mass degenerate bands were included.

Recently, using femtosecond midinfrared-induced luminescence Burr and Tang[40] have found that hole lifetime in spin-orbit split-off band of GaAs is $\tau_s=(50\pm15)$ fs. This value is shorter than the π-pulse length, about 200 fs at half maximum, in Fig. 1. The calculation were repeated with dissipation in the density-matrix equation taken into account with parameter values in Table I. Figure 2 shows the evolution of the distribution of holes having approximately the

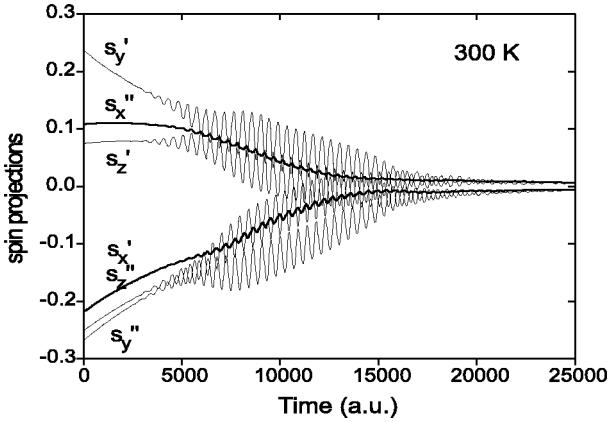

FIG. 3. Relaxation of hole spin projections at two randomly selected phase differences between degenerate heavy-mass band wave functions. $\mathbf{k_0}=0.2\times(-1,1,1)$ nm^{-1}.

same initial energy (the modulus of $\mathbf{k_0}$ was kept constant) as in Fig. 1 but at different directions of the wave vector characterized by polar $\theta°$ and azimuthal $\varphi°$ angles with respect to crystallographic axes. First of all, it should be noted that the maximum excitation of the split-off band has decreased by an order of magnitude and is about 0.1 now. Furthermore, the excitation character is insensitive to wave vector direction. Second, the decay of *s* population is very fast: the hole lifetime τ_s deduced from decrease of the *s* population in Fig. 2 is about 65 fs. This value agrees with the experiment.[40] Third, there remain small residual oscillations that are synchronous with field oscillations, even after the ensemble averaging over final scattering angles has been performed.

Figure 3 shows relaxation of projections of hole spin $\mathbf{s}=(s_x,s_y,s_z)$ for a hole having initial wave vector $\mathbf{k_0}=0.2\times(-1,1,1)$ nm^{-1}. The projections were calculated with combined, $J=\frac{3}{2}$ for *h* and *l* bands and $J=\frac{1}{2}$ for *s* band, angular momentum matrices, and time-dependent density matrix $\hat{\rho}$ at two fixed scattering angles but at a random initial phase difference $\Delta\phi_{ii}$. The phases $\Delta\phi_{ii}$ were included only in nondiagonal, $|\psi_{i1}\rangle\langle\psi_{i2}|$ and $|\psi_{i2}\rangle\langle\psi_{i1}|$, elements of $\hat{\sigma}_e$

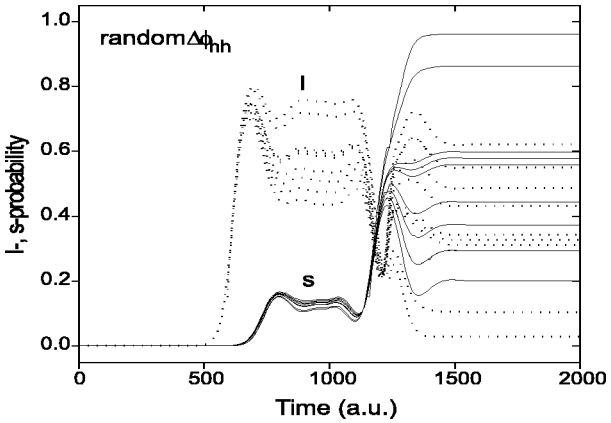

FIG. 4. Time dependence of the probabilities to detect the hole in *s* and *l* bands for randomly selected initial phase differences $\Delta\phi_{hh}$ between heavy-mass band degenerate wave functions. $t_f=2000$ a.u.$=48.4$ fs.

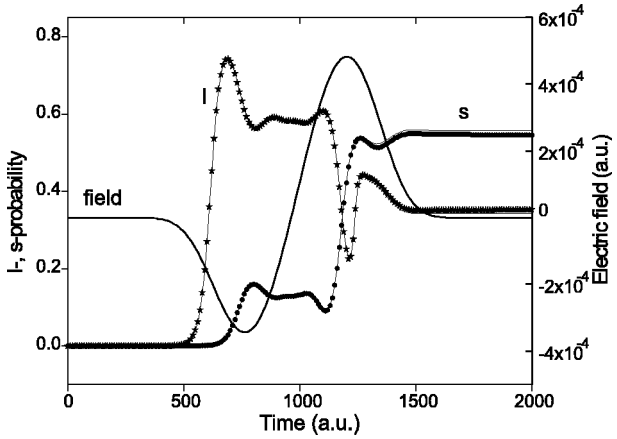

FIG. 5. Lines show the probabilities to detect the hole in *s* and *l* bands when the dissipation term in the density matrix is switched off. Points represent calculations with Schrödinger system and averaging over 200 random initial phase differences $\Delta\phi_{hh}$. The shape of the exciting field, $\mathbf{F(t)}=[F_x(t),0,0]$, is shown too.

that couple degenerate states only. The initial values for diagonal elements or probabilities $\sigma_{ii}=|\psi_i\rangle\langle\psi_i|$, where $i=s1,s2,l1,l2,h1,h2$, were assumed to be the same as in Fig. 2. Interband nondiagonal elements that connect *h*, *l*, and *s* bands were equated zero. From Fig. 3 it is clear that contrary to probabilities the spin projections do depend on the initial phase difference between degenerate wave functions, in this case mainly between *h*-band functions, since at equilibrium the hole population in this band predominates. The initial nonzero spin projections do not cancel out if ensemble averaging over final hole scattering angles is performed. Thus, Figs 1–3 demonstrate that in case of degenerate states an ensemble average over the final scattering states alone does not guarantee that all physical quantities will behave as one expects for a homogeneous semiconductor in equilibrium. In the remaining part of this section, results of simulation using pulses that are shorter than average hole momentum scattering time will be presented. Under these conditions long time coherence predominates in the transitions and the adiabatic approximation does not hold.

In Fig. 4 the family of curves shows the evolution of probability to find the hole in light-mass and split-off band calculated with GA and Schrödinger equation, while in Fig. 5 the curves show the evolution calculated with the density matrix when initial matrix is diagonal, $\hat{\sigma}_e=\mathrm{diag}\{0,0,0,0,0.5,0.5\}$ in the order of Eq. (9). In both figures the optimized pulse consists of one optical period. The optimized pulse is asymmetric with equal positive and negative amplitudes, respectively, 2.4×10^6 V/cm and 1.8×10^6 V/cm. It is seen that the final excitation probabilities $p_s(t_f)$ and $p_l(t_f)$, respectively, to *s* and *l* bands (Fig. 4) now strongly depend on phase difference $\Delta\varphi_{hh}$. At some $\Delta\varphi_{hh}$ values the excitation has a two step character—at first, the hole with high probability is excited to *l* band and then to *s* band—while the probability $p_s(t_f)$ may be close to one. The points in Fig. 5 represent averaged probabilities after integration of the Schrödinger system over 200 random phase differences. From these figures it is clear that the averaging

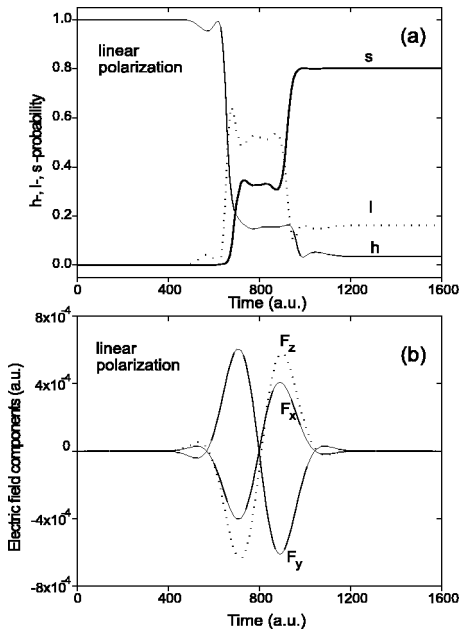

FIG. 6. (a) Valence-band occupation probabilities vs time for a hole with $\mathbf{k_0}=0.2\times(1,1,1)$ nm^{-1}. (b) The exciting electric-field components.

over initial phase differences of degenerate wave functions is equivalent to equating to zero matrix elements that couple degenerate bands in the initial density matrix.

Figure 6 shows the case where field polarization is different. It was found that in case of high intensity and ultrashort fields, in spite of valence-band anisotropy, similar picture is observed for this and other polarizations of the field after optimization. The effect of dissipation at $T=300$ K on excitation probabilities of holes having different wave-vector directions with respect of crystallographic axes, when $\hat{\sigma}_e$ is diagonal and when the electric-field shown in Fig. 6(b) has been used, is presented in Fig. 7. Figure 7(a) demonstrates that despite ultrafast decay of population from *s* band it is possible to reach high excitation probabilities, if coherent excitation with the optimized femtosecond pulses is used. In Fig. 7(b), the evolution of the probabilities to detect the hole in *l* band under same initial and excitation conditions is shown. The dependence on the angle in this case has an opposite character. In general, it has been observed that the coherent excitation of the *s* band coexists with the excitation of the *l* band at intermediate times. At this stage it is unclear whether this is associated with LK Hamiltonian or this property reflects a finite set of all possible electric-field shapes given by Eq. (11).

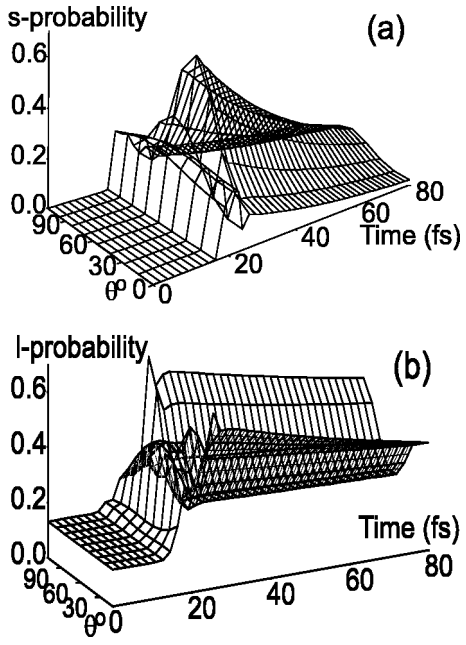

FIG. 7. Evolution of hole distribution in (a) split-off band and (b) light-mass band at different polar angles of the initial wave vector. The field is shown in Fig. 6(b). $T=300$ K.

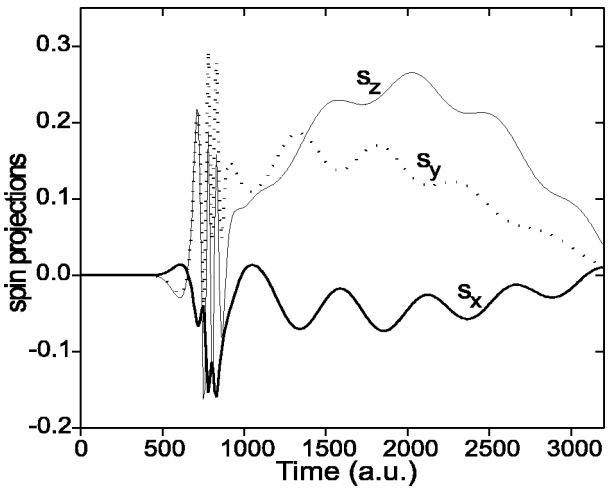

FIG. 8. Evolution of spin projections of subensemble of holes for which $\mathbf{k_0}=0.2\times(1,1,1)$ nm^{-1}. The electric field is the same as in Fig. 6(b). $T=300$ K.

Finally, Fig. 8 shows time dependence of spin projections, after averaging over final scattering angles for all possible scattering mechanisms, of the subensemble of holes having $\mathbf{k_0}=0.2\times(1,1,1)$ nm^{-1} at $t=0$. As in Fig. 7, nondiagonal elements of $\hat{\sigma}_e$ were assumed to be equal zero. Now, the subensemble of holes has zero initial spin. Figure 8 also shows that, due to the presence of strong spin-orbit interaction in GaAs, the hole spin changes in a very fast way during the action of the electric-field pulse and in the absence of the pulse relaxes back to an equilibrium in a spiral-like trajectory.

IV. DISCUSSION AND CONCLUSIONS

Excitation of the split-off valence band by subpicosecond infrared pulses was studied in *p*-GaAs in a limit of zero hole concentration. Numerical experiments have shown that in spite of very short lifetime (50–60 fs) of holes in the split-off band it is possible to achieve high excitation level, if excitation is coherent and the exciting pulse has an optimal shape. The light-mass band takes part in *h*-*s* transitions at intermediate times. Because hole scattering times in *l* band are

longer by an order of magnitude than in *s* band, the coherence of transitions is not destroyed. The dynamics of transitions induced by linearly polarized fields were presented. Calculations have also been done with circularly polarized femtosecond pulses, however, lower levels of *s*-band excitation were observed in this case.

It was found that the final transition probability and spin are sensitive to initial phase relations between degenerate wave functions, if duration of the exciting field in the Schrödinger equation is short enough. This property does not vanish if valence-band splitting due to linear-**k** terms is included in the Hamiltonian. However, the final population probabilities were found to be insensitive to phase relations between degenerate band wave functions if slow perturbation of the valence band, when the leading and trailing edges of the pulse consist of more than about five or more optical periods, was used. These results are in accordance with quantum evolution of a system under a slowly changing Hamiltonian—the so called adiabatic evolution (see, for example, discussion on this point in Ref. 39 and literature cited therein). Although in the considered case of *p*-GaAs the adiabatic evolution of the LK Hamiltonian is destroyed by fast hole intraband and interband scattering, nonetheless, the question remains what is a physical meaning of the phase differences $\Delta\varphi_{ii}$ between *i*th degenerate band wave functions. The optical transitions investigated in this paper take place in a homogeneous media, therefore, no spatial interference effects associated with hole wave function phase are expected. Numerical experiments have shown (Figs. 3 and 8) that $\Delta\phi_{ii}$ is intimately connected with an initial spin value and direction of the hole. Normally, one has to do either with electric or magnetic dipoles associated with transitions between states coupling different energy bands. However, in case of the valence band, due to strong spin-orbit interaction between the bands,[2] the LK Hamiltonian and the spin operator cannot be diagonalized simultaneously. This means that, in general, energy bands cannot be characterized by exact spin quantum numbers. By the same reason, during intervalence band transitions induced by an electric field, a part of the spin associated with the doubly degenerate band manifold is not conserved. This explains why the superposition of two degenerate wave functions of the valence band, for example, of heavy-mass band wave functions will generate spin dipole, the magnitude and direction of which depends on how degenerate wave functions are superimposed. By computer experiment it was checked that, indeed, the phase differences $\Delta\phi_{ii}$ in the Schrödinger equation (1) are related with nondiagonal density matrix elements that connect degenerate states $i=h,l,$ or *s*. It was shown that at a given initial wave vector these degenerate wave-function pairs yield nonzero contribution to the projections of the hole spin and, consequently, to transition probability the magnitude of which changes with $\Delta\phi_{ii}$ (Fig. 4). Thus, a unique solution of the time-dependent Schrödinger equation as an initial value problem requires certain postulates to be done as to phase relations between LK Hamiltonian degenerate wave functions what, in its turn, presupposes certain assumptions on absence or presence of nonzero spin dipole projections in a homogeneous semiconductor before the electromagnetic pulse is switched on. If one desires to calculate femtosecond transitions of hole distribution in an initially unpolarized medium, then one must take average over an ensemble of all the phase differences $\Delta\phi_{ii}$. Without performing such averaging one will implicitly assume some initial uncontrollable polarization of the medium. The simulation has shown (Fig. 5) that averaging over initial wave-function phases is equivalent to equating all nondiagonal matrix elements to zero in the density matrix $\hat{\sigma}$ that connect degenerate states.

Since the LK Hamiltonian is very complicated, various approximations are used in the literature to simplify it. The most popular of these reduce the LK Hamiltonian to 3×3 block-diagonal form with a unitary transformation or using some simplifying assumptions, for example, semiaxial[3,12] or spherical.[41] Such simplifications in the LK Hamiltonian automatically bring about modifications or restrictions on phase relations of degenerate spinor wave functions and, consequently, on hole initial spin. If averaging over all phase differences of the degenerate wave functions is not performed properly after a such simplification, nonzero magnetic dipoles are presupposed in the system. The paper shows that for general form of the LK Hamiltonian represented by Eqs. (2) and (3) the averaging over random initial phase differences is adequate to eliminate initial spin dipoles, which are connected with band degeneracy. Alternatively, one may start with the density-matrix equation and then equate zero those matrix elements that connect degenerate states.

In conclusion, from the joint analysis of the Schrödinger and density-matrix equations based on the LK Hamiltonian, it follows that the value of hole spin, apart from intervalence matrix elements, also depends on phase relations between doubly degenerate or nearly degenerate valence-band wave functions. The initial phase relations may be important in quantum control of femtosecond interband and spin-related excitation in doped bulk semiconductors and nanostructures, where strong spin-orbit interaction allows to control spin by time-varying electric fields.[29,30] From experimental and practical point of view, the phase differences between degenerate wave functions may serve as a kind of ''handles'' that allow to control quantum-mechanical hole spin. This may have important consequences in the ultrashort pulse spectroscopy of interband transitions and in ultrafast spintronics.

*Electronic address: dargys@uj.pfi.lt

[1] J. M. Luttinger and W. Kohn, Phys. Rev. **97**, 869 (1955).
[2] G. L. Bir and G. E. Pikus, *Symmetry and Strain-Induced Effects in Semiconductors* (Wiley, New York, 1974).
[3] E. P. O'Reilly, Semicond. Sci. Technol. **4**, 121 (1989).
[4] A. K. Ramdas and S. Rodriguez, Rep. Prog. Phys. **44**, 1297 (1981).
[5] A. Baldareschi and N. O. Lipari, Phys. Rev. B **9**, 1525 (1974).
[6] N. O. Lipari and M. Altarelli, Phys. Rev. B **15**, 4883 (1977).
[7] S. M. Kogan and A. P. Polupanov, Zh. Eksp. Teor. Fiz. **80**, 394 (1981).
[8] G. Bastard, J. A. Brum, and R. Ferreira, *Solid State Physics*, ed-

ited by H. Ehrenreich and D. Turnbull (Academic Press, New York, 1991), Vol. 44, p. 229.
[9] G. Goldoni and A. Fasolino, Phys. Rev. B **51**, 9903 (1995).
[10] R. H. Henderson and E. Towe, J. Appl. Phys. **79**, 2029 (1998).
[11] G. Hionis and G. P. Triberis, Superlattices Microstruct. **24**, 399 (1998).
[12] S. Rodriguez, J. A. López-Villanueva, I. Melchor, and J. E. Carceller, J. Appl. Phys. **86**, 438 (1999).
[13] E. Normantas, Fiz. Tekh. Poluprovodn. (S.-Peterburg) **16**, 630 (1982).
[14] S. Kakimoto and H. Watanabe, J. Appl. Phys. **85**, 1822 (1999).
[15] Y. Kajikawa, J. Appl. Phys. **86**, 5663 (1999).
[16] J. Taylor and V. Tolstikhin, J. Appl. Phys. **87**, 1054 (2000).
[17] K. I. Kolokolov, S. D. Baneslavski, N. Y. Minina, and A. M. Savin, Phys. Rev. B **63**, 195308 (2001).
[18] Y. Seko and A. Sakamoto, Jpn. J. Appl. Phys. **40**, 34 (2001).
[19] R. B. James and D. L. Smith, IEEE J. Quantum Electron. **18**, 1841 (1982).
[20] Yia-Chung Chang and R. B. James, Phys. Rev. B **39**, 12 672 (1989).
[21] D. A. Parshin and A. R. Shabaev, Zh. Eksp. Teor. Fiz. **92**, 1471 (1987).
[22] A. Dargys, J. Phys.: Condens. Matter **1**, 9637 (1989); **1**, 9653 (1989).
[23] A. Dargys and A. F. Rudolph, Phys. Status Solidi B **140**, 535 (1987).
[24] A. Dargys and R. Miliušytė, in *Proceedings of the Tenth International Conference on Noise*, edited by A. Ambrozy (Akadémiai Kiadó, Budapest, 1990), p. 91.
[25] J. L. Krause, D. H. Reitze, G. D. Sanders, A. V. Kuznetsov, and C. J. Stanton, Phys. Rev. B **57**, 9024 (1998).
[26] A. Dargys, Phys. Rev. B **64**, 235123 (2001).
[27] A. Dargys, Phys. Status Solidi B **219**, 401 (2000).
[28] A. Dargys, Opt. Commun. **206**, 123 (2002).
[29] R. D. R. Bhat and J. E. Sipe, Phys. Rev. Lett. **85**, 5432 (2000).
[30] M. J. Stevens, A. L. Smirl, R. D. R. Bhat, J. E. Sipe, and H. H. van Driel, J. Appl. Phys. **91**, 4382 (2002).
[31] B. A. Foreman, Phys. Rev. Lett. **86**, 2641 (2001).
[32] D. E. Goldberg, *Genetic Algorithm in Search, Optimization, and Machine Learning* (Addison-Wesley, Reading, MA, 1989).
[33] Z. Michalewicz, *Genetic Algorithms + Data Structures = Evolution Programs* (Springer-Verlag, Berlin, 1992).
[34] N. Bloembergen and Y. R. Shen, Phys. Rev. **133**, A37 (1964).
[35] N. Nintunze and M. A. Osman, Semicond. Sci. Technol. **10**, 11 (1995).
[36] G. E. Pikus and A. N. Titkov, in *Optical Orientation*, edited by F. Meier and B. P. Zakharchenya (Elsevier, North-Holland, 1984), Vol. 8, p. 73.
[37] N. S. Averkiev, L. E. Golub, and M. Willander, J. Phys.: Condens. Matter **14**, R271 (2002).
[38] A. Dargys and J. Kundrotas, *Handbook on Physical Properties of Ge, Si, GaAs, and InP* (Science and Encyclopedia Publishers, Vilnius, 1994).
[39] D. Kohen and D. J. Tannor, J. Chem. Phys. **98**, 3168 (1993).
[40] K. C. Burr and C. L. Tang, Appl. Phys. Lett. **74**, 1734 (1999).
[41] A. Dargys, Phys. Rev. B **59**, 4888 (1999).